

Fast proximity effect correction method using a pattern area density map

Fumio Murai, Haruo Yoda, Shinji Okazaki, Norio Saitou, and Yoshio Sakitani

Citation: *Journal of Vacuum Science & Technology B* **10**, 3072 (1992); doi: 10.1116/1.585931

View online: <http://dx.doi.org/10.1116/1.585931>

View Table of Contents: <http://scitation.aip.org/content/avs/journal/jvstb/10/6?ver=pdfcov>

Published by the AVS: Science & Technology of Materials, Interfaces, and Processing

Articles you may be interested in

[Proximity effect correction using pattern shape modification and area density map for electron-beam projection lithography](#)

J. Vac. Sci. Technol. B **19**, 2483 (2001); 10.1116/1.1410090

[Incorporating a corner correction scheme into enhanced pattern area density proximity effect correction](#)

J. Vac. Sci. Technol. B **19**, 1985 (2001); 10.1116/1.1396642

[Proximity effect correction using pattern shape modification and area density map](#)

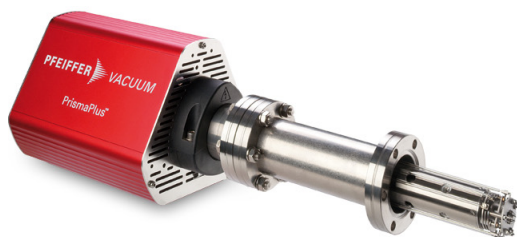
J. Vac. Sci. Technol. B **18**, 3150 (2000); 10.1116/1.1313576

[Enhanced pattern area density proximity effect correction](#)

J. Vac. Sci. Technol. B **17**, 323 (1999); 10.1116/1.590559

[Studies on correction accuracy of proximity effect for the pattern area density method in electron beam direct writing](#)

J. Vac. Sci. Technol. B **14**, 3870 (1996); 10.1116/1.588684



PrismaPlus™ RGA

- Modular design
- Sensitive and stable
- Powerful software for Intelligent operation

PFEIFFER  **VACUUM**

Fast proximity effect correction method using a pattern area density map

Fumio Murai

Central Research Laboratory, Hitachi Ltd., 185 Kokubunji, Tokyo, Japan

Haruo Yoda

Instrument Division, Hitachi Ltd., 312 Katsuta, Ibaraki, Japan

Shinji Okazaki and Norio Saitou

Central Research Laboratory, Hitachi Ltd., 185 Kokubunji, Tokyo, Japan

Yoshio Sakitani

Instrument Division, Hitachi Ltd., 312 Katsuta, Ibaraki, Japan

(Received 26 May 1992; accepted 23 July 1992)

This article proposes a new method for proximity effect correction that utilizes newly developed hardware. The correction algorithm modifies the exposure dose for each exposure point by referring to a pattern area density map. The only additional process in this method is virtual exposure to make the map. The virtual exposure is carried out once at the first use of the large-scale integration circuit pattern and can be processed in only 30 s. The pattern area density map makes it possible to correct the proximity effect from the lower-level patterns by the new map calculated from the two maps of lower level and exposing level. The usefulness of this method is verified by experiments using model patterns.

I. INTRODUCTION

The progress of ultra-large-scale integration circuits (ULSIs) depends largely on microlithography. The first 64-Mb dynamic random access memory (DRAM) was developed using electron-beam (e-beam) direct writing.¹ However, photolithography using a phase-shifting technique is going to take the place in production. The main difficulty in e-beam direct writing is low throughput. Cell projection is a potential method of increasing throughput.^{2,3} The degradation of resolution by the proximity effect is another obstacle for practical use of e-beam lithography. Correcting this effect usually requires a very long calculation time. Although subsidiary exposure methods like GHOST, which was proposed by Owen and Rissman,⁴ require no complex calculation, they need a second exposure with a defocused beam. These correction methods result in a long data preparation time or low throughput in exposure.

To make processing faster, the correction can be calculated by dedicated hardware. This can be done using the algorithm for the optimum dose and a pattern area density map. This article describes a new method for high-speed correction for the proximity effect and our experimental results.

II. CORRECTION ALGORITHM

A. Basic equation for correction

The deposition energy profile due to a point exposure is expressed as the well-known double Gaussian expression⁵ as

$$f(r) = \frac{1}{1+\eta} \left[\frac{1}{\beta_f^2} \exp\left(-\frac{r^2}{\beta_f^2}\right) + \frac{\eta}{\beta_b^2} \exp\left(-\frac{r^2}{\beta_b^2}\right) \right], \quad (1)$$

where r is the distance from the irradiation point, β_f is the forward-scattering range, β_b is the backscattering range, and η is the ratio of the backscattering energy to the

forward-scattering energy (hereafter η is simply called the backscattering ratio). The deposition energy due to pattern exposure is obtained by integrating Eq. (1) over the pattern. The result can be expressed as a combination of error functions.

A high-energy electron beam makes the proximity effect correction simpler.⁶ For example, the backscattering range β_b of 50-keV electrons is about 10 μm , which results in very gradual variation of backscattered energy. Although the exact forward-scattering range β_f is difficult to measure, Monte Carlo simulation predicts that a 50-keV electron beam with 0.05- μm beam blur has a large dose latitude in fabricating a 0.2- μm line even on a high backscattering substrate.⁷ This suggests that a small change in optimum dose is required in the subquarter micron range. Under these conditions, Eq. (1) becomes very simple. Suppose the effect of backscattering within a small region is roughly constant, then the energy level due to backscattering depends only on the backscattering ratio η and the sum of the areas of nearby patterns. This means that the optimum exposure dose can be determined from the pattern area density in each small region and the backscattering ratio of the substrate, assuming that the forward-scattering range is small enough. The algorithm in this article assumes that the optimum exposure dose of each e-beam shot is determined so that the average level of the deposition energy at an exposed point and unexposed point is constant at any pattern area density.

Figure 1 shows a uniform pattern density. The deposition energy at an unexposed point E_b is caused only by backscattering from nearby patterns, giving

$$E_b = C_1 \alpha \eta D, \quad (2)$$

where α is the pattern area density, D is the exposure dose, and C_1 is a constant. At an exposed point, the deposition

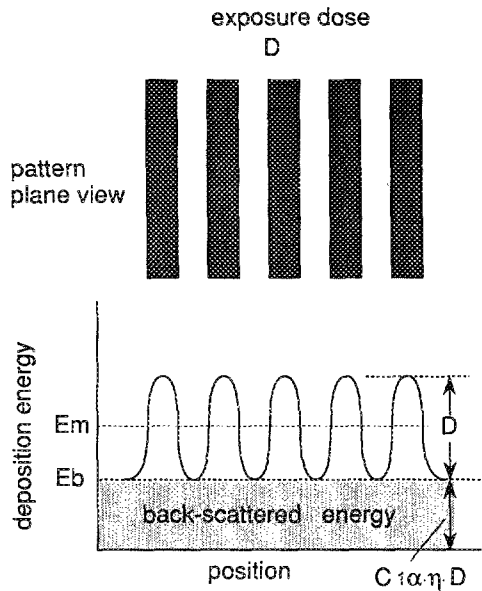


FIG. 1. Determination of the optimum doses.

energy E_b is caused by both forward scattering and back-scattering. Adding the forward-scattering component to Eq. (2):

$$E_e = C_1 D + E_b = C_1 (1 + \alpha \eta) D. \quad (3)$$

The middle of the energy level E_m is obtained by averaging Eqs. (2) and (3):

$$E_m = (1/2)(E_b + E_e) = (C_1/2)(1 + 2\alpha \eta) D. \quad (4)$$

To make the energy level E_m constant at any pattern area density, the exposure dose D must satisfy the following relation:

$$D = C_2 / (1 + 2\alpha \eta), \quad (5)$$

where $C_2 (= 2E_m / C_1)$ is a constant.

B. Correction procedure

This method uses specially designed hardware to calculate the proximity effect correction using the basic Eq. (5). The hardware and the data flow are shown in Fig. 2. The special feature of this method is that it stores a map of the pattern area density for the whole of the LSI chip to be exposed.

First, virtual exposure is executed. The LSI patterns are partitioned with a mesh of fixed size in which the back-scattered energy is roughly constant. Then the pattern area density (α) is calculated for each small region. (Here, "small region" means the region partitioned with a mesh.) After smoothing the area densities in two dimensions, these data (α') are stored in the map memory. The detail of the smoothing operation will be discussed later. This virtual exposure is executed only once at the first use of a new LSI pattern. As the calculation of the area density and the smoothing operation can be processed by the fast multipliers and arithmetic and logic unit (ALU), the pattern area density map can be formed within half a minute.

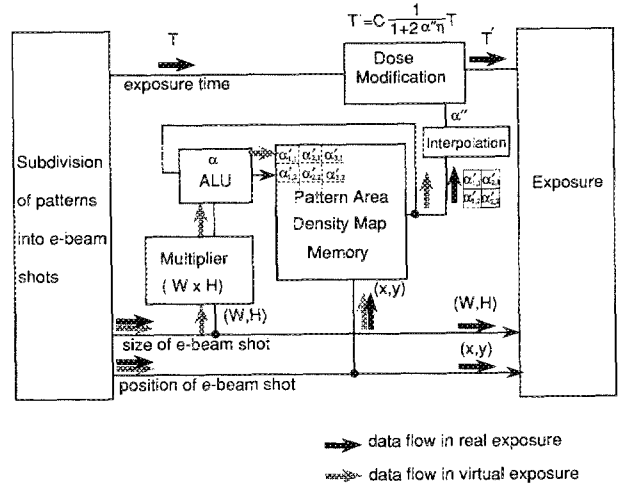


FIG. 2. Configuration of correction hardware.

The determination of the mesh size is important because the correction error depends on the mesh size and smoothing range. Though small mesh size and wide smoothing range are desirable for precise correction, mesh size is chosen to be roughly equal to the backscattering range (β_b) due to the limited amount of map memory.

When this correction scheme is used together with cell projection exposure, there is no information about the pattern area in pattern data. In this case the area of a cell electron beam is given separately and is added to an area density map when the cell pattern is called.

For real exposure to wafers, the pattern is divided into many e-beam shots whose sizes are less than the maximum allowable e-beam size. The area density (α') is interpolated using the four area densities nearest to each exposure shot, and the exposure dose is modified according to Eq. (5) and the interpolated area density (α''). As this correction is processed during the exposure, the throughput is not reduced.

C. Smoothing of the area density map

When LSI patterns are partitioned with a mesh of fixed size, the mesh boundary may divide an original region with the same geometrical pattern into several small regions with different area densities. Another problem is that the optimum dose by Eq. (5) is calculated assuming a uniform pattern density. For real LSI patterns, we must take into account the fact that nearby small regions may have different pattern area densities.

These problems can be drastically reduced by correcting the actual pattern area densities nearby meshes. This is schematically shown in Fig. 3. The resulting corrected area density in the (i,j) mesh is extrapolated from the adjacent 3×3 meshes by the following equation:

$$\alpha'(i,j) = \sum_{l=i-1}^{l=i+1} \sum_{m=j-1}^{m=j+1} a(l,m) \alpha(l,m), \quad (6)$$

where $\alpha(i,j)$ and $\alpha'(i,j)$ are the original and corrected pattern area densities. In Fig. 3, $a(i,j)$ is the energy depo-

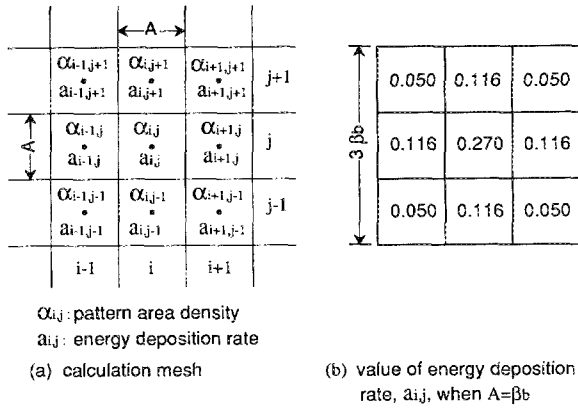


FIG. 3. Smoothing of the area density map in 3x3 small regions.

sition rate which is defined as the ratio of the deposition energy in the small region (i,j) to the total deposition energy by the exposure in the small region (l,m). When the mesh size is A, the energy deposition rate a(i,j) can be obtained from Eq. (1), neglecting the forward scattering. This gives

$$a(i,j) = \left[\operatorname{erf} \left(\frac{A}{2\beta_b} \right) \right]^2, \tag{7}$$

$$a(i \pm 1, j) = a(i, j \pm 1) = \frac{1}{2} \left[\operatorname{erf} \left(\frac{A}{2\beta_b} \right) \right] \left[\operatorname{erf} \left(\frac{3A}{2\beta_b} \right) - \operatorname{erf} \left(\frac{A}{2\beta_b} \right) \right], \tag{8}$$

$$a(i \pm 1, j \pm 1) = \frac{1}{4} \left[\operatorname{erf} \left(\frac{3A}{2\beta_b} \right) - \operatorname{erf} \left(\frac{A}{2\beta_b} \right) \right]^2. \tag{9}$$

When the mesh size A is chosen to be the backscattering range β_b , the energy deposition ratios, e.g., a(i,j) are as shown in Fig. 3(b). The value a(i+1,j)=0.116, e.g., means that 11.6% of the pattern in area (i+1,j) can be considered as existing in area (i,j) to decide the doses of the pattern in that area. [In Fig. 3(b), $\sum a(i,j)=0.934$, which means 93.4% of the deposition energy is considered. Smoothing in 5x5 meshes is preferable for higher accuracy.]

D. Correction of proximity effect from lower-level patterns

The proximity effect is not only caused by the patterns in the same level. When aluminum wiring patterns are exposed on a patterned tungsten layer, both aluminum and tungsten levels must be taken into account in proximity effect correction. This is because the backscattering ratio of the substrate depends on the heavy metal patterns on it.

As shown in Fig. 4 the backscattering comes from both tungsten patterns and other regions. The area density and backscattering ratio of lower-level patterns are put to α_s and η_s . The backscattering from lower-level patterns is $\alpha_s \eta_s D$, and backscattering from another area is $(1-\alpha_s) \eta D$ when the whole area is exposed. Thus the effective overall backscattering ratio is $[\alpha_s \eta_s + (1-\alpha_s) \eta]$, and con-

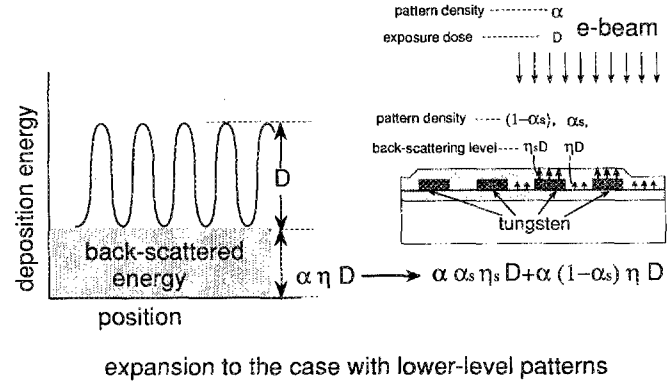


FIG. 4. Correction of proximity effect from lower-level patterns. α : pattern area density of exposing level; α_s : pattern area density of lower level; η : backscattering ratio of the material without lower-level patterns; and η_s : backscattering ratio of the material of lower-level patterns.

sequently the energy level by backscattering is the sum of the following two terms:

$$E_n = C_1 \alpha \alpha_s \eta_s D + C_1 \alpha (1 - \alpha_s) \eta D. \tag{10}$$

The optimum dose is similarly obtained to Eq. (5):

$$D = C_3 / \{ 1 + 2\alpha [\eta + \alpha_s (\eta_s - \eta)] \}, \tag{11}$$

where C_3 is a constant.

If a new map is produced from the maps of the lower level and exposing level of Eq. (11), the proximity effect from the patterns of both levels can be corrected. The mesh size of this area density map must be determined by the smaller backscattering range of either the lower level or exposing level. Other procedures for correction operation are the same as in Sec. II B.

E. Data processing time

As the dose correction is carried out simultaneously with the exposure, this method requires only data processing time for preparing the pattern area density map. The time for preparing this map is the time for calculating the pattern area density plus the time for smoothing the area density map. The first depends on the total shot counts of electron beam and the smoothing time depends on the number of meshes, and thus depends on the chip size and mesh size.

The data volume to be handled depends only on the number of meshes, because a mesh has only one pattern area density. When a mesh size of 10 μm is chosen in a 400-mm² chip, map memory stores 4×10^6 data which corresponds to 4 MB in our system. The value is not changed even when lower-level patterns are taken into account.

The cell projection² method can be introduced for memory LSIs to reduce the shot number. As mentioned in Sec. II B, area densities of cell patterns are given separately in the calculation within a mesh. For a memory LSI with a 400-mm² chip area, 1×10^7 e-beam shots per chip including a cell projection beam with $5 \times 5\text{-}\mu\text{m}^2$ size and variable-shaped beam exposure, it takes about 9 s to make the map. Because application specific integration circuits (ASICs)

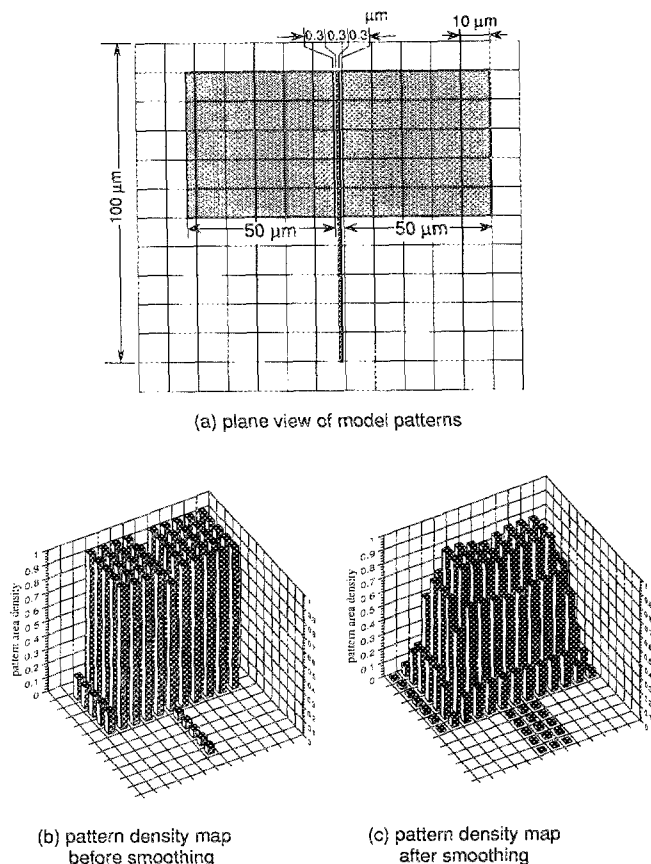


FIG. 5. Model patterns for experiments and pattern area density maps.

have less repeated unit patterns, the total number of e-beam shots is 4×10^7 for a 100-mm^2 chip area with single use of a variable-shaped beam exposure. In this case the estimated map preparation time is about 14 s. For further increase of shot counts in future LSIs, the required time for proximity effect correction will be < 30 s.

III. EXPERIMENTS

The algorithm for this method was evaluated by experiments, using a variable-shaped e-beam lithography system HL750D (Hitachi Ltd.). The acceleration voltage was 50 kV, the current density was 10 A/cm^2 , and the maximum shot size was $2 \times 2 \text{ μm}^2$. Negative tone e-beam resist SAL®601 (Shipley) was used with 0.3-μm thickness. The proximity parameters were determined by a point exposure method.⁸ The backscattering range was $\beta_b = 9.7 \text{ μm}$ and the backscattering ratio was $\eta = 0.74$ at these exposure conditions.

The model patterns are shown in Fig. 5(a). The proximity effect was evaluated by measuring the linewidth of the patterns of $0.2, 0.3,$ and 0.5 μm wide placed partially between two pads of $50 \times 50 \text{ μm}$, which is much larger than the backscattering range. The mesh size of the map was set at 10 μm , which is nearly equal to β_b . Figures 5(b) and 5(c) show the pattern area density map before and after smoothing. Although the fixed mesh size gives different area densities at the right-most and left-most small regions, these differences are reduced by smoothing. The

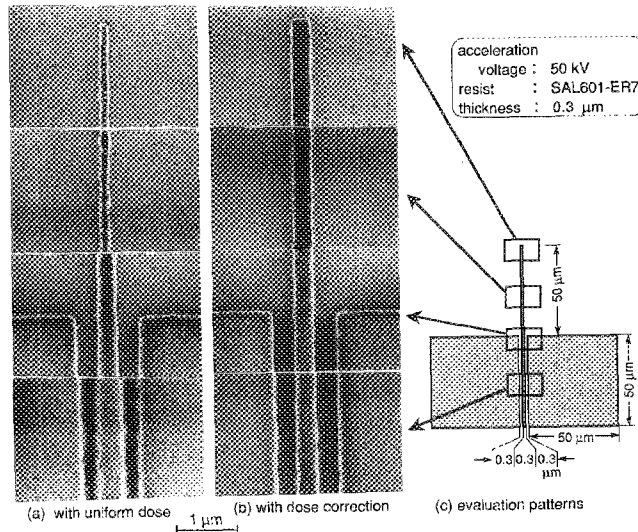


FIG. 6. Evaluation experiments using model patterns.

exposure dose of each e-beam shot was modified using Eq. (5) and the area densities in Fig. 5(b). The scanning electron microscopy (SEM) micrographs of the developed resist patterns are shown in Fig. 6 with uniform dose and corrected dose. It is clear that the linewidth is constant from the dense region to the isolated region. Figure 7 shows the measured linewidths of the three patterns at different points. With the pattern density map and a single correction equation [Eq. (5)], linewidth errors can be suppressed to under 0.02 μm for a wide range of pattern densities and pattern sizes.

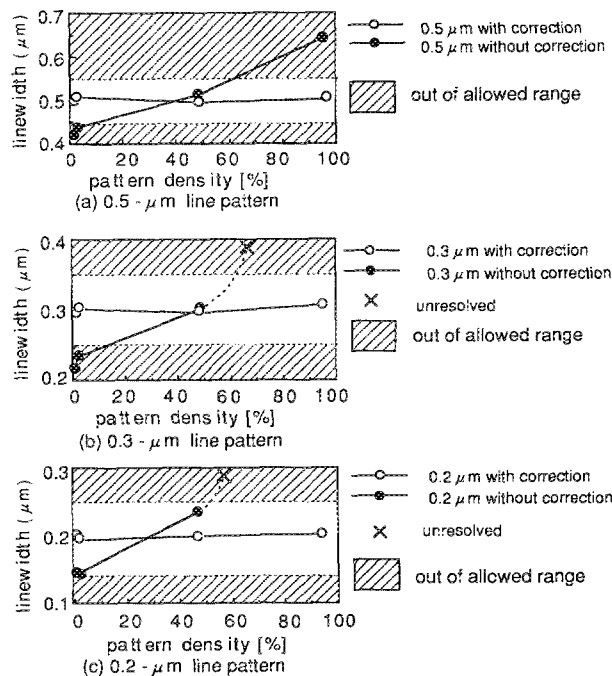


FIG. 7. Measured linewidth for various line patterns and pattern area densities.

IV. CONCLUSIONS

We have proposed a new method to correct the proximity effect. The correction algorithm modifies each exposure dose of the subdivided e-beam shot depending on the pattern area density near the shot. The algorithm is implemented in newly developed hardware comprised of area density map memory, fast multipliers, and ALU. The data processing time using this method is estimated at about 9 s for a memory LSI with a chip area of 400 mm² using a combination of cell projection and a variable-shaped beam. It takes 14 s for a ASIC with an area of 100 mm² with single use of a variable-shaped beam. The pattern area density map can also correct the proximity effect from the lower-level patterns. Experiments using model patterns show that the method is accurate down to 0.2- μ m patterns.

ACKNOWLEDGMENTS

The authors wish to thank to A. Moniwa for her help in Monte Carlo simulation, T. Yamamoto for his help in operating the electron-beam system, Y. Kato for her help in the simulation and experiments, and T. Nishida for his useful comments on the manuscript.

¹F. Murai, Y. Nakayama, I. Sakama, T. Kaga, Y. Nakagome, Y. Kawamoto, and S. Okazaki, *Jpn. J. Appl. Phys.* **11**, 2590 (1990).

²Y. Nakayama, S. Okazaki, N. Saiton, and H. Wakabayashi, *J. Vac. Sci. Technol. B* **8**, 1836 (1990).

³H. Yasudo, K. Sakamoto, A. Yamada, and K. Kawashima, *Jpn. J. Appl. Phys.* **30**, 3098 (1991).

⁴G. Owen and P. Rissman, *J. Appl. Phys.* **54**, 3573 (1983).

⁵T. H. P. Chang, *J. Vac. Sci. Technol.* **12**, 1271 (1989).

⁶T. Abe, N. Ikeda, H. Kusakabe, R. Yoshikawa, and T. Takigawa, *J. Vac. Sci. Technol. B* **7**, 1524 (1989).

⁷A. Moniwa and S. Okazaki, *Jpn. J. Appl. Phys.* **30**, 3093 (1991).

⁸F. Murai, S. Okazaki, N. Saito, and M. Dan, *J. Vac. Sci. Technol. B* **5**, 105 (1987).